The Journal *of* Immunology

The Effects of Dendritic Cell Hypersensitivity on Persistent Viral Infection

Jennifer S. Tsau, Xin Huang, Chen-Yen Lai and Stephen M. Hedrick

---

References   This article **cites 69 articles**, 31 of which you can access for free at:
http://www.jimmunol.org/content/200/4/1335.full#ref-list-1

Why *The JI*? Submit online.

- **Rapid Reviews! 30 days*** from submission to initial decision

- **No Triage!** Every submission reviewed by practicing scientists

- **Fast Publication!** 4 weeks from acceptance to publication

*average

Subscription   Information about subscribing to *The Journal of Immunology* is online at:
http://jimmunol.org/subscription

Permissions   Submit copyright permission requests at:
http://www.aai.org/About/Publications/JI/copyright.html

Email Alerts   Receive free email-alerts when new articles cite this article. Sign up at:
http://jimmunol.org/alerts

The Effects of Dendritic Cell Hypersensitivity on Persistent Viral Infection

Jennifer S. Tsau,* Xin Huang,[†] Chen-Yen Lai,[†] and Stephen M. Hedrick*,[†]

Caspase-8 (CASP8) is known as an executioner of apoptosis, but more recent studies have shown that it participates in the regulation of necroptosis and innate immunity. In this study, we show that CASP8 negatively regulates retinoic acid–inducible gene I (RIG-I) signaling such that, in its absence, stimulation of the RIG-I pathway in dendritic cells (DCs) produced modestly enhanced activation of IFN regulatory factor 3 with correspondingly greater amounts of proinflammatory cytokines. In addition, mice lacking DC-specific CASP8 (dcCasp8$^{-/-}$ mice) develop age-dependent symptoms of autoimmune disease characterized by hyperactive DCs and T cells, spleen and liver immunopathology, and the appearance of Th1-polarized CD4$^+$ T cells. Such mice infected with chronic lymphocytic choriomeningitis virus, an RNA virus detected by RIG-I, mounted an enhanced lymphocytic choriomeningitis virus–specific immune response as measured by increased proportions of Ag-specific CD4$^+$ T cells and multicytokine-producing CD4$^+$ and CD8$^+$ T cells. These results show that CASP8 subtly modulates DC maturation, which controls the spontaneous appearance of autoimmune T cells while simultaneously attenuating the acquired immune system and its potential to control a persistent viral infection. *The Journal of Immunology*, 2018, 200: 1335–1346.

Dendritic cells (DCs) bridge innate and adaptive immunity by acting as sentries that detect invading pathogens. In addition, they act as professional APCs capable of potently activating Ag-specific T cells (1, 2). As a consequence of pathogen recognition, DCs undergo a program of maturation that includes Ag presentation by cell-surface MHC molecules and enhanced expression of essential costimulatory molecules including CD80 and CD86 (1–3). In the steady state, immature DCs instead contribute to immune tolerance by presenting self-antigens to autoreactive lymphocytes, leading to their anergy, deletion, or conversion to induced regulatory T cells (4, 5). DCs that become mature in the absence of infection can thus provoke an immune response to self Ags, as seen in autoimmune diseases from multiple sclerosis and type 1 diabetes to systemic lupus erythematosus (SLE) (6). A role for DCs in human SLE pathogenesis is supported by the finding that DCs from SLE patients have been shown to upregulate CD86 expression independent of activating stimuli (7).

Immature DCs use endocytic pathogen recognition receptors to detect infectious agents that bear pathogen-associated molecular patterns and, upon uptake and processing, present associated oligopeptides to T cells (8). For example, DCs can detect viral dsRNA using retinoic acid–inducible gene I (RIG-I)-like receptors such as RIG-I (9, 10). Initiation of RIG-I signaling leads to the formation of a mitochondrial signaling complex consisting of MAVS, FADD, TRADD, TANK, and RIPK1, activation of IFN regulatory factors (IRFs) 3 and 7, and production of type I IFNs (IFN-I), cytokines with pleiotropic effects in immunity and disease (9, 11–15). IFN-I constitute important antiviral cytokines and are a major stimulus for DC activation, but they are also considered a key driver of disease development in SLE (16, 17).

The cysteine–aspartic acid protease, caspase-8 (CASP8), known for its canonical role in executing death receptor-mediated apoptosis, also inhibits necroptosis, an alternative form of programmed cell death that occurs under CASP8-deficient conditions (18, 19). In many cell types, when CASP8 is inhibited, necroptosis can be triggered by the same stimuli that initiate apoptosis, such as death receptor ligation or TCR stimulation, and is mediated by the kinases RIPK1 and RIPK3 (20–30). However, $Casp8^{-/-}$ DCs are not more prone to dying upon treatment with the death receptor ligands TNF-α or FasL, suggesting that DCs lacking CASP8 are not sensitized toward necroptosis (31, 32).

In addition to its inhibitory effect on necroptosis, CASP8 is also a negative regulator of RIG-I signaling. CASP8 inhibits the formation of the RIG-I–dependent mitochondrial signaling complex by cleaving RIPK1, and a loss of CASP8 in nonhematopoietic cells resulted in enhanced phosphorylation of IRF3 (33). CASP8 was also shown to directly cleave IRF3, leading to its degradation (34). Subsequent studies showed that $Casp8$ ablation in DCs led to increased production of proinflammatory cytokines, due to a loss of inhibition of either RIPK3-mediated NLRP3 inflammasome activation, or RIPK1- and MyD88-mediated DC activation (31, 32). Mice with $Casp8^{-/-}$ DCs were also shown to develop an age-dependent autoimmune disease that was not prevented by deleting RIPK3, suggesting a non-necroptotic driver of this autoimmunity (32). Indeed, DCs and macrophages appear to be unique in that a loss of $Casp8$ in these cell types does not appear to potentiate necroptosis, unlike in other tissues (26, 28–30, 35). We chose to investigate the role of RIG-I signaling in disease development of these mice, as the overall contribution of the RIG-I pathway to the function of $Casp8^{-/-}$ DCs is unclear.

*Division of Biological Sciences, Molecular Biology Section, University of California, San Diego, La Jolla, CA 92093; and †Cellular and Molecular Medicine, University of California, San Diego, La Jolla, CA 92093

ORCID: 0000-0002-8935-5187 (X.H.).

Address correspondence and reprint requests to Prof. Stephen M. Hedrick, Molecular Biology Section, University of California, San Diego, 9500 Gilman Drive, La Jolla, CA 92093. E-mail address: shedrick@ucsd.edu

The abbreviations used in this article: BMDC, bone marrow–derived DC; CASP8, caspase-8; cDC, conventional DC; DC, dendritic cell; GC, germinal center; IFN-I, type I IFN; IRF, IFN regulatory factor; LCMV, lymphocytic choriomeningitis virus; LCMV Cl13, LCMV clone 13; MHCII, MHC class II; Nec-1, Necrostatin-1; NP, nucleoprotein; p.i., postinfection; PI, propidium iodide; poly(I:C), polyinosinic-polycytidylic acid; RIG-I, retinoic acid–inducible gene I; SLE, systemic lupus erythematosus; Tfh, follicular helper T; WT, wild type.

In this study we addressed the role of CASP8 in specific pathogen-free and disease conditions and, specifically, how the subtle modulation of one aspect of the innate immune response changes the balance between spontaneous autoimmune pathology and the efficacy of viral clearance. We show that mice with $Casp8^{-/-}$ DCs develop an age-dependent hyperactivation of DCs and T cells and associated immunopathology, with a predominance of IFN-γ–producing Th1 cells. Along with age-dependent autoimmunity, the loss of $Casp8$ in DCs also allowed mice to mount an enhanced response to chronic viral infection, which was characterized by less exhausted, Ag-specific T cells and lower viral loads. These immunity characteristics correlated with DCs that were more sensitive to RIG-I stimulation in vitro. Thus, by regulating just one aspect of DC activation, CASP8 acts as a rheostat to dial in a well-tempered immune system, albeit one that is less efficacious.

Materials and Methods
Mice

Mice in which exon 3 of $Casp8$ is flanked by loxP sites (B6.129-Casp8tm1Hed) (backcrossed to C57BL/6J, $n > 10$) (36) were crossed to $Cd11cCre$ mice [B6.Cg-Tg(Itgax-cre)1-1Reiz/J] (37) to generate $Casp8^{flox/flox}$ $Cd11cCre$ mice. These mice are referred to as $dcCasp8^{-/-}$. SMARTA transgenic mice [TCR transgenes specific for H2-A^b bound with lymphocytic choriomeningitis virus (LCMV) gp$_{61–80}$] (38) were a gift from A. Goldrath, University of California, San Diego. Animal work was performed according to University of California, San Diego guidelines.

Viral infections

Mice 6–10 wk old were infected i.v. via the retroorbital sinus with 2×10^6 PFU LCMV clone 13 (LCMV Cl13). Virus was grown, identified, quantified, and titered by plaque assay as previously described (39). LCMV-specific ELISAs were performed as previously described (40).

Flow cytometry

Spleens were harvested from mice and treated with Collagenase D (Roche) at 37°C for 20 min. Splenic single-cell suspensions were made and incubated with the indicated fluorochrome-conjugated Abs. For intracellular staining of Foxp3 and cytokines (IFN-γ, TNF, and IL-2), FoxP3 Fix/Perm kit (eBioscience) was used. For intracellular staining of p-IRF3, Cytofix Fixation Buffer and Perm Buffer III (BD Biosciences) were used. LCMV-specific T cells were examined with MHC class II (MHCII) (H2-A^b gp66) and MHCI (H2-D^b gp33, H2-D^b gp276, H2-D^b nucleoprotein [NP]396) tetramers obtained from the National Institutes of Health Tetramer Core Facility (Emory University). All Abs for surface and intracellular cytokine staining were purchased from eBioscience, BioLegend, or BD Biosciences. p-IRF3 Ab was purchased from Cell Signaling Technology.

Data were collected on an LSRFortessa (BD Biosciences) and analyzed with FlowJo software (Tree Star).

Flow cytometry gating strategy

For DCs, the splenocytes were gated to 1) exclude T cells, B cells, NK cells, macrophages, and monocytes (antibodies to CD3, CD19, CD49b, F4/80 and Ly6C, respectively); 2) exclude plasmacytoid DCs (B220$^+$CD11c^{lo}) and include conventional DCs (cDCs) (B220$^-$CD11c^{hi}); 3) subset CD11b$^+$ CD8$^-$ (CD11b$^+$) versus CD11b$^-$CD8$^+$ (CD8$^+$) cDCs. For p-IRF3 expression studies, CD11b$^+$ cDCs were placed in further subsets of CD86^{hi} and CD86^{lo} populations.

In vitro stimulations

In total, 10^6 splenocytes were isolated and stimulated for 1 h with PMA (10 ng/ml) and ionomycin (1 μM) to assess CD4 T cell skewing, or LCMV peptides gp$_{33–41}$ (0.5 μM) or gp$_{61–80}$ (2 μg/ml) to assess cytokine production, after which monensin (eBioscience) was added for an additional 3.5 h, for a total stimulation of 4.5 h.

Polyinosinic-polycytidylic acid transfections

Three to four spleens per genotype were pooled to isolate 2.7×10^5 CD11c$^+$ cells per well to at least 90% purity according to EasySep CD11c Positive Selection Kit with Spleen Dissociation Medium (Stemcell). For CD86 upregulation and proinflammatory cytokine measurements, CD11c$^+$ cells were transfected with short-length polyinosinic-polycytidylic acid [poly(I:C)]-LyoVec (InvivoGen)

for 20 h at the indicated concentrations, according to the manufacturer's instructions. LPS was added at 0.1 μg per well. Cytokines were assessed in the cell supernatant by cytometric bead assay (BioLegend). For DC coculture assay, 0.9×10^5 CD45.1$^+$ CD45.2$^+$ wild-type (WT) CD11c$^+$ cells were cocultured with 1.8×10^5 CD45.2$^+$ control or $Casp8^{-/-}$ CD11c$^+$ cells in the presence of transfected short-length poly(I:C)-LyoVec at the indicated concentrations for 16 h. Total viability was assessed with the Zombie Aqua Fixable Viability Kit (BioLegend). For cell death assays, CD11c$^+$ cells were stimulated for 16 h with anti-Fas, Jo2 clone (0.2 mg/ml; BD Biosciences) or short-length poly(I:C)-LyoVec at the indicated concentrations, with or without pretreatment for one hour with Necrostatin-1 (Nec-1) (30 μM; Enzo Life Sciences), and then stained with annexin V and propidium iodide (PI) (eBioscience), according to the manufacturer's instructions. For p-IRF3 analysis by flow cytometry, CD11c$^+$ cells were transfected with short-length poly(I:C)-LyoVec (5 μg/ml) for the indicated lengths of time. Poly(I:C)-LyoVec preparations and media used were endotoxin free.

Histopathology

Paraffin-embedded spleen and liver sections were stained with H&E. Splenic white and red pulp areas were quantified by ImageJ software (National Institutes of Health).

SMARTA adoptive transfer

LCMV-specific CD45.1$^+$ CD45.2$^+$ transgenic SMARTA CD4$^+$ T cells were isolated by microbeads using negative selection to at least 85% purity (Miltenyi Biotec). Then, 5000 SMARTAs were transferred i.v. into recipient mice 1 d prior to LCMV Cl13 infection.

Bone marrow–derived DC differentiation

Bone marrow was harvested from femurs and tibias, resuspended in complete media containing 20 ng/ml each of GM-CSF and IL-4 (PeproTech), and placed in six-well plates at a density of 1×10^6 cells per ml. Two thirds of the media was replaced on days 3, 5, and 7 with fresh media plus GM-CSF and IL-4. Nonadherent cells were harvested on day 9, and negative selection with microbeads (Miltenyi Biotec) was used to remove F4/80$^+$, Ly6C$^+$, and B220$^+$ cells. Bone marrow–derived DCs (BMDCs) were then transfected for 0, 1, 2, or 4 h with short-length poly(I:C)-LyoVec and total cell lysates were isolated.

Immunoblot analysis

Equal amounts of protein from total BMDC lysates were resolved by 4–12% NU PAGE Bis-Tris gel (Invitrogen) and were transferred to Immobilon-P polyvinylidene difluoride membrane (Millipore) by semidry transfer (Bio-Rad). Blots were incubated overnight at 4°C with primary Abs to p-IRF3 (Cell Signaling), total IRF3 (Cell Signaling) or LaminB (Santa Cruz), then incubated for 1 h at 25°C with the appropriate HRP-conjugated secondary Ab. Bands were visualized by SuperSignal West Femto Maximum Sensitivity Substrate (Thermo Fisher Scientific).

Results
Mice with $Casp8^{-/-}$ DCs develop an age-dependent autoimmune phenotype

To investigate the contribution of CASP8 in the regulation of DCs, mice with a $Casp8^{flox/flox}$ allele were crossed with $Cd11cCre$ mice to generate $Casp8^{flox/flox}Cd11cCre$ conditional knockout mice (hereafter referred to as $dcCasp8^{-/-}$ mice). Deletion of exon 3 of $Casp8$ in CD11c$^+$ splenocytes from $dcCasp8^{-/-}$ mice was validated by PCR (Fig. 1A). These mice displayed higher proportions of hyperactive CD11b$^+$ and CD8$^+$ cDCs at 3 mo of age, as assessed by the expression of CD86 (Fig. 1B), and cDCs from $dcCasp8^{-/-}$ mice remained hyperactive through 14-plus mo of age. To determine whether the hyperactivation seen in cDCs was reflected in the population of T cells, we assessed the status of T cells by enumerating previously activated (CD44^{hi}CD62^{lo}) versus naive (CD44^{lo}CD62L^{hi}) T cells found in the spleen and blood. As shown, CD4$^+$ T cells from $dcCasp8^{-/-}$ mice generated increased proportions of activated T cells at 3 mo of age, whereas activated CD8$^+$ T cells were not increased until 6 mo of age (Fig. 1C). The proportion of previously activated T cells in control ($Casp8^{flox/flox}$)
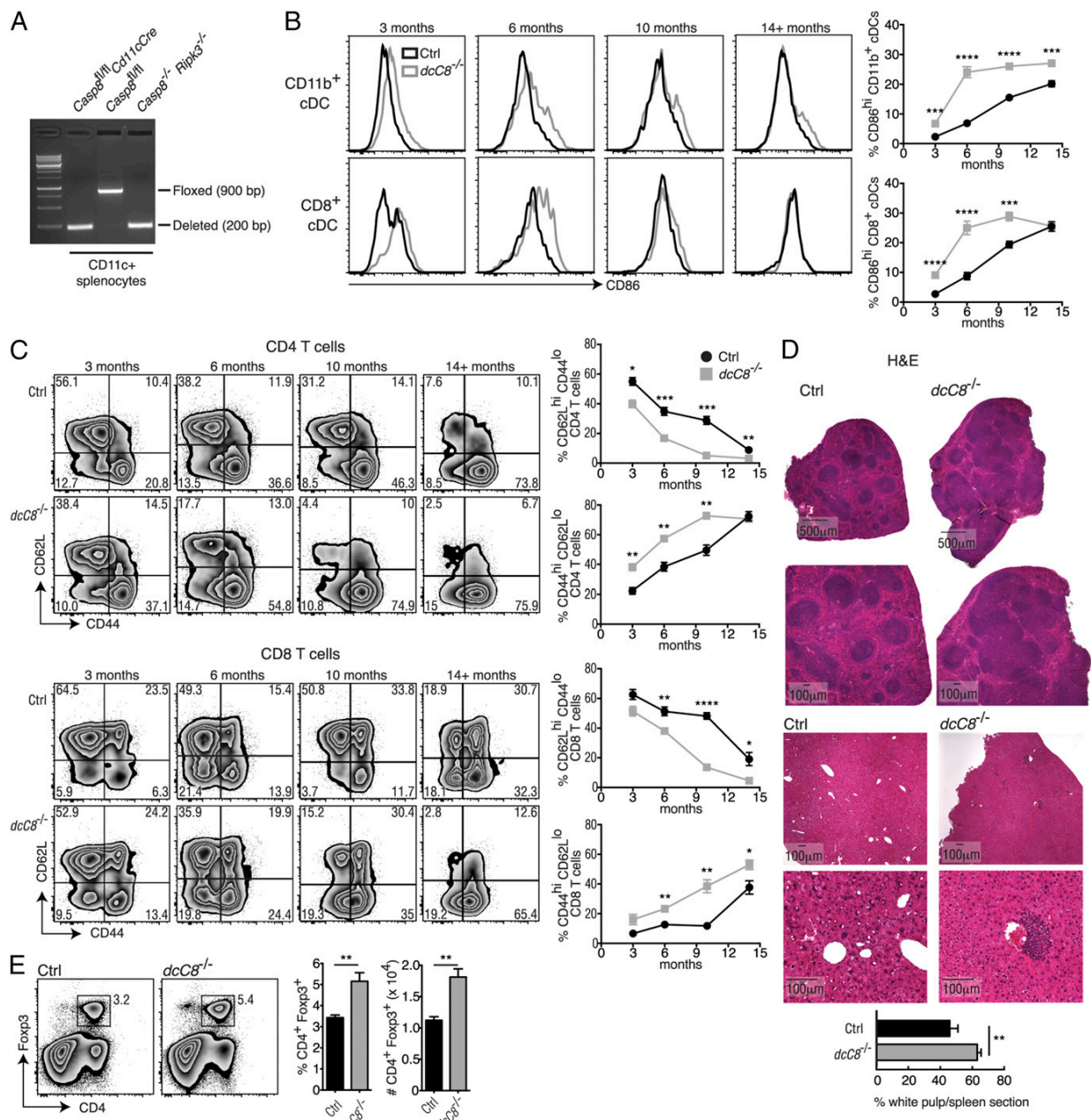
FIGURE 1. Phenotype of aged $dcCasp8^{-/-}$ mice. (**A**) Deletion of exon 3 of CASP8 was assessed in CD11c$^+$ splenocytes from $Casp8^{fl/fl}$ (control), $Casp8^{fl/fl}$ $Cd11cCre$ ($dcCasp8^{-/-}$), and $Casp8^{-/-}$ $Ripk3^{-/-}$ mice by PCR. (**B**) The expression of CD86 in splenic cDCs from control and $dcCasp8^{-/-}$ mice was determined at 3, 6, 10, and 14+ mo (left), and the percentage of cDCs expressing high levels of CD86 is depicted (right). (**C**) The expression of CD62L and CD44 in splenic and blood T cells from control and $dcCasp8^{-/-}$ mice was determined at 3, 6, 10, and 14+ mo (left), and the percentage of T cells that were naive (CD62L^{hi}CD44^{lo}) or activated (CD62L^{lo}CD44^{hi}) is depicted (right). (**D**) Spleens and livers from 10 mo old control and $dcCasp8^{-/-}$ mice were sectioned and stained with H&E. The percentage of white pulp area per spleen section in control versus $dcCasp8^{-/-}$ mice is depicted (right). (**E**) The expression of Foxp3 in splenic CD4$^+$ T cells from 10 mo old control and $dcCasp8^{-/-}$ mice was determined by percentage (left) and absolute number per spleen (right). Data for (A), (B), (D), and (E) are representative of three independent experiments for each time point, with $n = 4$. Data for (C) are representative of 16 mice. Error bars represent SEM. $*p \leq 0.05$, $**p \leq 0.01$, $***p \leq 0.001$, $****p \leq 0.0001$.

mice increased with age; however, this was substantially accelerated in $dcCasp8^{-/-}$ mice for both CD4$^+$ and CD8$^+$ subsets.

We next determined whether the hyperactive cDCs and T cells in aged $dcCasp8^{-/-}$ mice had an effect on organ immunopathology. Spleens from aged $dcCasp8^{-/-}$ mice displayed a disrupted splenic architecture, as demonstrated by an expansion of white pulp (Fig. 1D). Livers from aged $dcCasp8^{-/-}$ mice showed an increase

in polymorphic infiltrates similar to the infiltrating leukocytes seen in autoimmune mice with Fas-deficient cDCs (41) (Fig. 1D). Because aged $dcCasp8^{-/-}$ mice appeared to display signs of autoimmunity, we examined whether the number of Foxp3$^+$ regulatory T cells was diminished. On the contrary, we found increased percentages and numbers of Foxp3$^+$ regulatory T cells in 10 mo old $dcCasp8^{-/-}$ mice (Fig. 1E).

CD4⁺ T cells from aged dcCasp8⁻/⁻ mice skew toward a Th1 phenotype

Many autoimmune diseases are characterized by the emergence of a particular CD4⁺ Th subset characterized by its hallmark cytokine. For example, IFN-γ–producing Th1 cells are more prevalent in the peripheral blood of human SLE patients (42). To determine whether CD4⁺ T cells in aged *dcCasp8⁻/⁻* mice were polarized for a specific Th subset, we stimulated splenocytes in vitro with PMA and ionomycin for 4 h and analyzed the appearance of diagnostic cytokines. The results showed an increased subset of CD4⁺ T cells from aged *dcCasp8⁻/⁻* mice that produced IFN-γ, when compared with control mice, whereas the proportions of CD4⁺ T cells producing IL-4 and IL-17 were similar (Fig. 2).

Young adult dcCasp8⁻/⁻ mice mount an enhanced Ag-specific T cell response to chronic viral infection

Because specific pathogen-free *dcCasp8⁻/⁻* mice display accelerated development of activated cDCs and T cells over time, we determined how *dcCasp8⁻/⁻* mice would respond to a viral infection. Taking into account our observation that *dcCasp8⁻/⁻* mice developed a detectable increase in activated cDCs and CD4⁺ T cells by 3 mo of age, we infected young adult (6–10 wk old) mice before the appearance of phenotypic manifestations of the *Casp8* deletion. Specifically, we wished to determine whether *dcCasp8⁻/⁻* mice would mount an exaggerated response to viral infection as a result of enhanced cDC activation and Ag presentation to T cells.

LCMV is an RNA virus that is detected by RIG-I (43). Inoculation of C57BL/6 mice with 10⁶ PFU LCMV Cl13, the chronic form of LCMV, results in a long and persistent viral infection (39, 44). A characteristic of the CD4⁺ and CD8⁺ T cell response is the induction of multiple negative feedback pathways starting day 12 postinfection (p.i.), and these mechanisms appear to prolong the viral infection while lessening the associated immunopathology (45, 46). Previous work has shown that removal of negative regulation can be readily detected (47, 48). In addition, LCMV Cl13 is able to establish a chronic infection partly because it selectively infects and suppresses DCs (49), and thus, enhanced DC function might be expected to mitigate this form of LCMV virulence.

Upon infection of 6–10 wk old *dcCasp8⁻/⁻* mice with LCMV Cl13, the expansion of Ag-specific T cell responses was examined using tetramers specific for the major immunodominant CD4⁺ and CD8⁺ T cell epitopes. We found that *dcCasp8⁻/⁻* mice had higher proportions of H2-Aᵇ gp66⁺ CD4⁺ T cells at days 8 and 15 p.i. (Fig. 3A). *dcCasp8⁻/⁻* mice had similar proportions of H2-Dᵇ gp33⁺ CD8⁺ and H2-Dᵇ gp276⁺ CD8⁺ T cells from days 8 to 30 p.i., but interestingly, *dcCasp8⁻/⁻* mice had larger percentages of H2-Dᵇ NP396⁺ CD8⁺ T cells at days 8 and 30 (but not 15) p.i. (Fig. 3A). Overall, *dcCasp8⁻/⁻* mice possessed substantially higher frequencies of gp66-specific CD4⁺ T cells compared with control mice early in the infection, and this would be predicted to have an important effect on the expansion of CD8⁺ T cells and the clearance of virus.

T cells from chronically infected dcCasp8⁻/⁻ mice retain effector function

T cells achieve their antiviral effector function, in part, by producing cytokines such as IFN-γ and TNF. We assessed the ability of T cells from LCMV Cl13–infected *dcCasp8⁻/⁻* mice to produce IFN-γ and TNF upon restimulation with either CD4⁺ or CD8⁺ T cell LCMV-specific peptides (gp$_{61–80}$ and gp$_{33–41}$, respectively). The results showed that, consistent with the increased frequency of LCMV-specific T cells, a higher proportion of CD4⁺ T cells from *dcCasp8⁻/⁻* mice were polyfunctional and produced both IFN-γ and TNF at days 8 and 15 p.i. (Fig. 3B), and a higher proportion of CD8⁺
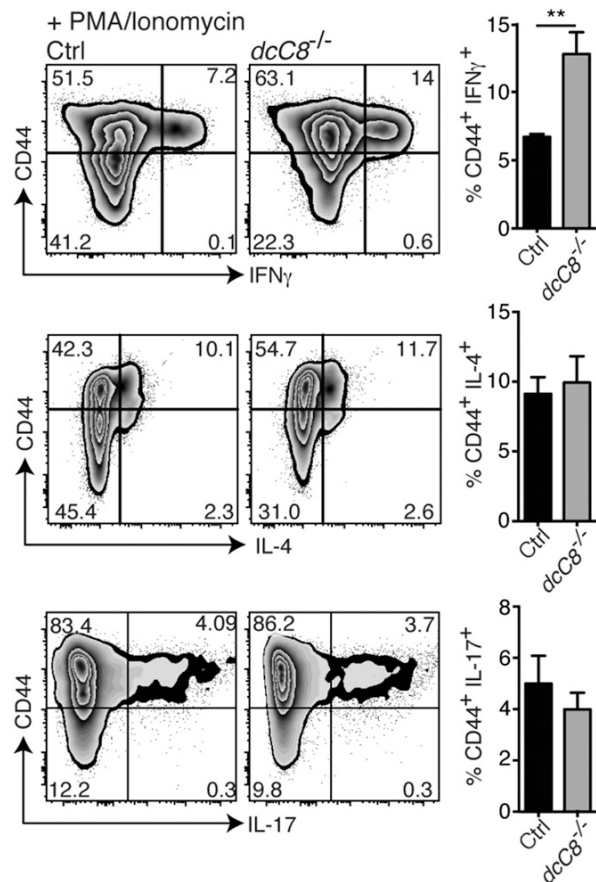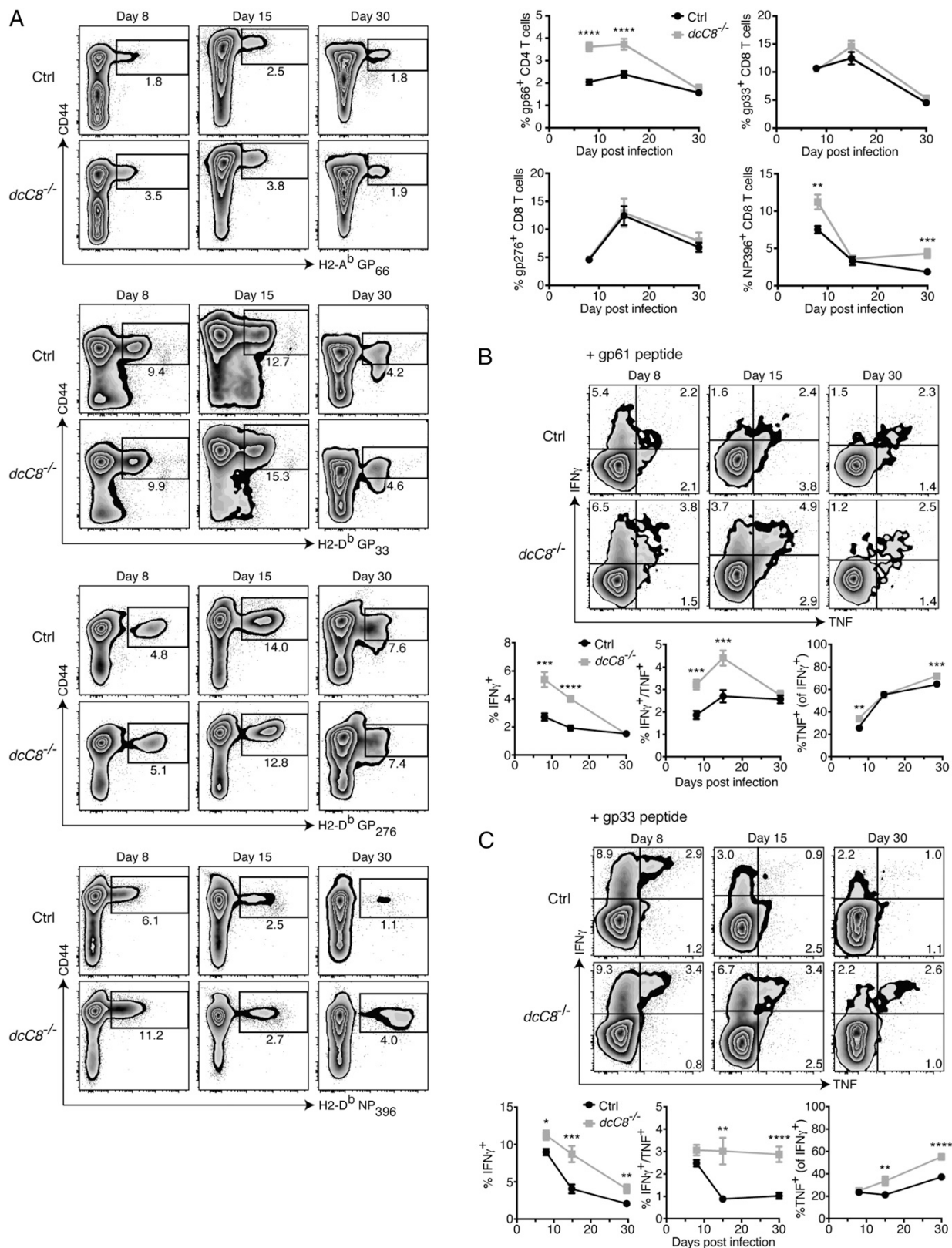

FIGURE 2. CD4⁺ T cells from aged *dcCasp8⁻/⁻* mice skew toward a Th1 phenotype. Splenocytes from 10 mo old control and *dcCasp8⁻/⁻* mice were tested for the expression of IFN-γ, IL-4, and IL-17 by intracellular staining. The percentage of CD44⁺ CD4⁺ T cells expressing IFN-γ, IL-4, or IL-17 is depicted (right). Data are representative of three independent experiments, with *n* = 4. Error bars represent SEM. **$p \leq 0.01$.

T cells from *dcCasp8⁻/⁻* mice were polyfunctional and produced both IFN-γ and TNF at days 15 and 30 p.i. (Fig. 3C). Taken together, these results suggest that chronically infected *dcCasp8⁻/⁻* mice have an early (days 8–15 p.i.) enhancement in the CD4⁺ T cell response, and a late (days 15–30 p.i.) enhancement in the CD8⁺ T cell response.

The effect of DC-specific Casp8 deletion on T cell exhaustion and viral clearance

Because we had seen more effector CD4⁺ and CD8⁺ T cells from *dcCasp8⁻/⁻* mice compared with control mice, we investigated whether T cells from *dcCasp8⁻/⁻* mice expressed differential levels of the inhibitory receptor PD-1, which is upregulated during T cell exhaustion (45). Analysis showed that H2-Aᵇ gp66⁺ CD4⁺ T cells from *dcCasp8⁻/⁻* mice expressed lower amounts of PD-1 by both median fluorescence intensity and the percentage of PD-1ʰⁱ expressing cells at day 30 p.i. (Fig. 4A). Similar results were found analyzing H2-Dᵇ gp33⁺ CD8⁺ T cells from *dcCasp8⁻/⁻* mice.

Because *dcCasp8⁻/⁻* mice possessed T cells that retained the ability to produce antiviral cytokines and were less exhausted at day 30 p.i., there was a possibility that virus load would be correspondingly reduced. Consistent with the time-course of T cell expansion and effector function, *dcCasp8⁻/⁻* mice displayed lower viral loads in serum, liver, and kidney at day 30 p.i. as measured by plaque assay (Fig. 4B, 4C).

FIGURE 3. Young adult $dcCasp8^{-/-}$ mice mount an enhanced T cell response to chronic LCMV. Control and $dcCasp8^{-/-}$ mice were infected with LCMV Cl13. After 8, 15, and 30 d, spleen cells were harvested and analyzed. (**A**) Representative analysis of CD44$^+$ CD4$^+$ T cells with H2-A^b gp66 tetramers and CD44$^+$ CD8$^+$ T cells with H2-D^b gp33, gp276, or NP396 tetramers (left). The accumulation of data are depicted (upper right). (**B** and **C**) Splenocytes were stimulated in vitro with either (B) gp$_{61–80}$ (CD4) or (C) gp$_{33–41}$ (CD8) peptide and the expression *(Figure legend continues)*

*dcCasp8^{−/−} mice have more Ag-specific follicular helper
T cells and higher levels of IgG2a Ab a month after chronic
infection*

Whereas WT mice clear an LCMV Cl13 infection (in lymphoid tissues) in 2–3 mo, mice lacking CD4$^+$ T cells do not clear the virus for over 4 mo, which appears to be due to the importance of CD4$^+$ T cells both in providing help to CD8$^+$ T cells and in promoting LCMV-specific Ab responses (50–52). Because we saw an enhanced LCMV-specific CD4$^+$ T response in *dcCasp8^{−/−}* mice, we examined whether the Ab response was likewise enhanced. Analyses showed that *dcCasp8^{−/−}* mice had greater proportions of H2-A^b gp66$^+$ CD4$^+$ follicular helper T (Tfh) cells at day 30 p.i. (Fig. 4D). Unexpectedly, we found that *dcCasp8^{−/−}* mice had substantially fewer germinal center (GC) B cells as measured by the expression of GL-7 and Fas (53) (Fig. 4E). GC B cells can differentiate into plasmablasts, which then form Ab-producing plasma cells. Yet, despite the reduction of GC B cells in *dcCasp8^{−/−}* mice, these mice trended toward having higher frequencies of plasmablasts (MHCII$^+$CD138$^+$) and plasma cells (CXCR4$^+$ CD138$^+$) (54). Additionally, at day 30 p.i. *dcCasp8^{−/−}* mice had higher levels of LCMV-specific IgG2a Ab, which is the isotype preferentially driven by increased IFN-γ (55). No differences in the amounts of LCMV-specific total IgG or IgG1 Abs were found (Fig. 4F).

The discrepancy between increased numbers of Tfh cells, increased Abs, but reduced GC B cells has not been resolved. Although the increased frequency of plasmablasts and plasma cells in *dcCasp8^{−/−}* mice was not statistically significant, it could help explain why *dcCasp8^{−/−}* mice have increased Tfh cells and increased LCMV-specific Abs. A chronic viral infection could accelerate the disruption of splenic architecture observed in uninfected aged *dcCasp8^{−/−}* mice (Fig. 1D), leading to a loss of splenic structure required for GC B cell formation. For example, although Lupus-prone MRL.*Fas^{lpr}* mice spontaneously develop GCs, they are lost over time and are no longer detectable in 6 mo old mice, perhaps due to the collapse of splenic architecture (56).

*LCMV-specific CD4 T cells from chronically infected
dcCasp8^{−/−} mice have enhanced expansion and effector
function*

To address the possibility that pre-existing hyperactivated CD4$^+$ T cells in *dcCasp8^{−/−}* mice contribute to the larger proportion of either H2-A^b gp66$^+$ CD4$^+$ T cells or IFN-γ/TNF–producing CD4$^+$ T cells in these mice (Fig. 3A, 3B), we adoptively transferred CD4$^+$ T cells from SMARTA transgenic mice into control and *dcCasp8^{−/−}* recipients followed by infection with LCMV Cl13. SMARTA mice have CD4$^+$ T cells specific for the gp$_{61–80}$ epitope of LCMV (38). We found that CD45.1$^+$CD45.2$^+$ SMARTA CD4$^+$ T cells transferred into *dcCasp8^{−/−}* hosts expanded to a greater degree in the blood at day 5 p.i. (Fig. 5A), and in the spleen at day 8 p.i. (Fig. 5B). When we examined the ability of SMARTA CD4$^+$ T cells from *dcCasp8^{−/−}* hosts to produce effector cytokines upon restimulation with the CD4$^+$ T cell LCMV-specific peptide (gp$_{61–80}$), we found that a higher proportion of SMARTA CD4$^+$ T cells from *dcCasp8^{−/−}* mice produced either IFN-γ alone, both IFN-γ and TNF, or both IFN-γ and IL-2, a finding consistent with the enhanced expansion of these cells in *dcCasp8^{−/−}* hosts (Fig. 5C). These results show that *dcCasp8^{−/−}* mice promote an enhanced expansion of naive T cells.

RIG-I stimulation hyperactivates cDCs lacking Casp8

We hypothesized that, in *dcCasp8^{−/−}* mice, both the age-dependent autoimmune phenotype and the enhanced response to chronic infection resulted from the loss of negative regulation of RIG-I signaling by CASP8 in cDCs. To directly test this, we activated RIG-I in *Casp8^{−/−}* cDCs by transfecting them with short-length poly (I:C), which is a surrogate for dsRNA and is specifically detected by RIG-I (57). We isolated splenic CD11c$^+$ cells from control and *dcCasp8^{−/−}* mice and transfected them with increasing doses of poly (I:C), then assessed the upregulation of the costimulation molecule CD86. We found that both CD11b$^+$ and CD8$^+$ cDCs upregulated CD86 to a greater degree than control cDCs in a poly(I:C) dose-dependent manner (Fig. 6A).

To determine whether *Casp8^{−/−}* cDCs hyperactivate due to a cell-intrinsic or cell-extrinsic mechanism, we cocultured *Casp8^{−/−}* and WT CD11c$^+$ cells in the presence of transfected poly(I:C). The results indicated that the hyperactivation of *Casp8^{−/−}* cDCs was cell extrinsic, as CD45.1$^+$CD45.2$^+$ WT cDCs cocultured with CD45.2$^+$ *Casp8^{−/−}* cDCs upregulated CD86 to a greater degree than when cocultured with CD45.2$^+$ control cDCs (Fig. 6B).

To directly assess whether this cell-extrinsic effect could be the result of *Casp8^{−/−}* cDCs producing more IFN-I upon RIG-I stimulation, we measured levels of IFN-β in the supernatant of poly(I:C)-transfected CD11c$^+$ cells. Surprisingly, we found that the supernatant of *Casp8^{−/−}* CD11c$^+$ cells contained significantly higher levels of IFN-β at only one concentration of transfected poly(I:C) compared with control supernatant (Fig. 6C). However, when we assessed the levels of several other proinflammatory cytokines, IFN-γ, TNF-α, IL-6, and MCP-1 were all found to be upregulated in the supernatant of *Casp8^{−/−}* CD11c$^+$ cells in response to increasing doses of transfected poly(I:C) (Fig. 6C), consistent with the cell-extrinsic DC hyperactivation mechanism predicted by Fig. 6B.

cDCs lacking Casp8 are not sensitized to necroptosis

Loss of *Casp8* in a variety of cell types leads to necroptosis, an alternative mode of programmed cell death that occurs when a cell receives death stimuli in the face of apoptosis inhibition (24, 25, 28). Immature DCs become mature upon coculture with cells undergoing necrosis or exposure to necrotic cell supernatant, likely due to the release of danger-associated molecular patterns during necrosis, but they do not mature when cultured with apoptotic cells or apoptotic cell supernatant (58).

To investigate whether necroptosis of *Casp8^{−/−}* cDCs could contribute to the hyperactivation of these cells, we first used a membrane permeable dye to compare levels of total cell death in control and *Casp8^{−/−}* poly(I:C)-transfected CD11c$^+$ cells, and found that the numbers of live control or *Casp8^{−/−}* cDCs per well were comparable (Fig. 6D). Next, we labeled poly(I:C)-transfected CD11c$^+$ cells with annexin V and PI and assessed the frequency of necroptotic cell death (annexin V$^+$PI$^+$). Whereas both control and *Casp8^{−/−}* cDCs (CD11b$^+$ or CD8$^+$ subsets) displayed greater numbers of annexin V$^+$PI$^+$ cells upon ligation of the death receptor Fas (by addition of anti-Fas Ab), neither control nor *Casp8^{−/−}* cDCs had an increase in the frequency of annexin V$^+$PI$^+$ cells upon poly(I:C) transfection (Fig. 6E). We infer that the increase in annexin V$^+$PI$^+$ cells in anti-Fas treated cDCs was due to late apoptosis, not necroptosis, as this cell death was triggered

---

of IFN-γ and TNF was assessed by intracellular staining (top). The percentage of CD44$^+$ CD4$^+$ and CD8$^+$ T cells that produce either IFN-γ alone, both IFN-γ and TNF, or TNF in addition to IFN-γ is depicted (bottom). Data are averaged from three independent experiments measuring at least 12 mice per group (A) or 10 mice per group (B). Error bars represent SEM. *$p ≤ 0.05$, **$p ≤ 0.01$, ***$p ≤ 0.001$, ****$p ≤ 0.0001$.
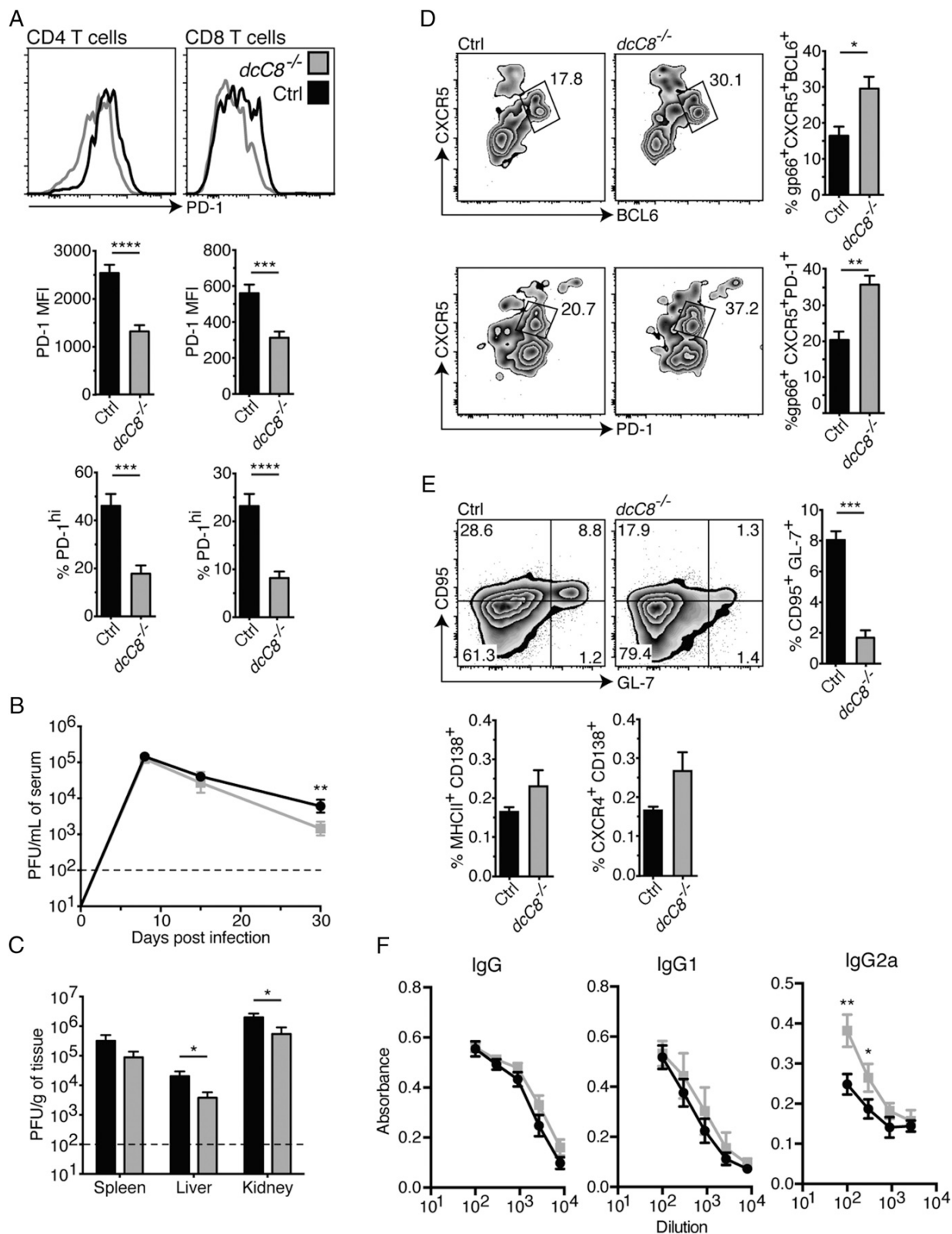
FIGURE 4. Phenotype of chronically infected young adult $dcCasp8^{-/-}$ mice. Control (black) and $dcCasp8^{-/-}$ (gray) 6–10 wk old mice were infected with LCMV Cl13. After 30 d, various organs and blood were harvested and analyzed. (**A**) The expression of PD-1 in H2-A^b gp66$^+$ CD4$^+$ or H2-D^b gp33$^+$ CD8$^+$ splenic T cells was assessed. The PD-1 median fluorescence intensity (MFI) and percentage of cells expressing high levels of PD-1 is depicted (bottom). Virus titers were determined (plaque assays) in (**B**) serum, (**C**) spleen, liver, and kidney. (**D**) The expression of CXCR5 and BCL6 or PD-1 in gp66$^+$ CD44$^+$ CD4$^+$ T cells was assessed, and the percentage of CXCR5^{hi}BCL6^{hi} and CXCR5^{hi}PD-1^{hi} cells is depicted (right). *(Figure legend continues)*
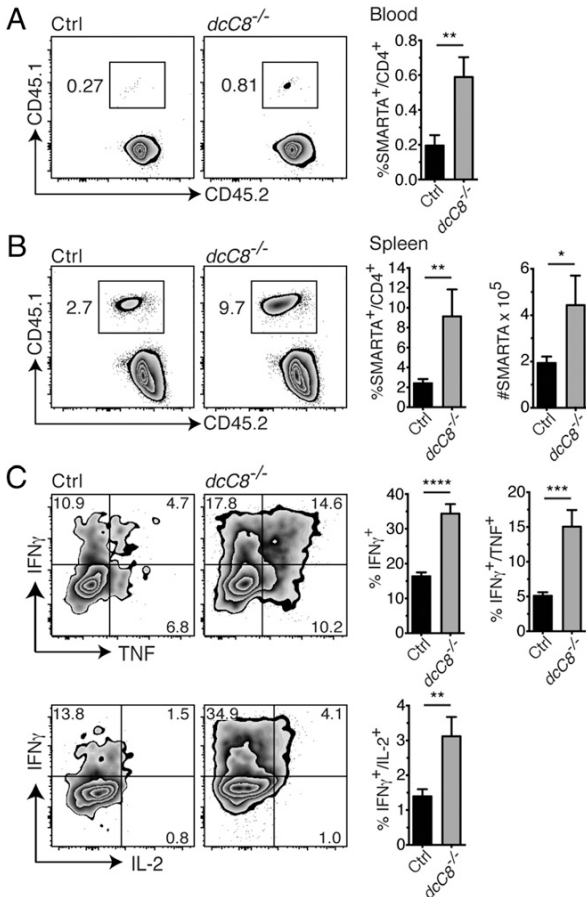
FIGURE 5. SMARTA T cells transferred into chronically infected $dcCasp8^{-/-}$ mice display great effector function. LCMV-specific CD45.1$^+$ CD45.2$^+$ transgenic CD4$^+$ T cells (SMARTA) were transferred i.v. 1 d prior to LCMV Cl13 infection. (**A**) The frequency of blood CD4$^+$ T cells that were SMARTA was assessed at day 5 p.i. (**B**) The frequency and number of spleen CD4$^+$ T cells that were SMARTA was assessed at day 8 p.i. (**C**) Splenocytes isolated at day 8 p.i. were stimulated with gp$_{61-80}$ (CD4) peptide and assessed for the expression of IFN-γ, TNF-α, and IL-2 by SMARTA CD4$^+$ T cells by intracellular staining (left). The percentage of SMARTA CD4$^+$ T cells that produce either IFN-γ alone, IFN-γ, and TNF-α, or IFN-γ and IL-2 is depicted (right). Data for (A and B) depict at least 10 pooled mice per group, and data for (C) depict at least 8 pooled mice per group taken from two to three independent experiments. Error bars represent SEM. *$p \leq 0.05$, **$p \leq 0.01$, ***$p \leq 0.001$, ****$p \leq 0.0001$.

by Fas signaling yet was not inhibited by the addition of Nec-1, an inhibitor of RIPK1. Thus, $Casp8^{-/-}$ cDCs do not appear to undergo necroptosis when death receptor signaling is triggered, consistent with a previous report (32).

BMDCs lacking Casp8 have enhanced IRF3 activation upon RIG-I stimulation

We originally predicted that the hyperactivation phenotype of $Casp8^{-/-}$ DCs was due to a loss of negative regulation of IRF3.

Thus, we measured whether levels of p-IRF3 in poly(I:C)-transfected $Casp8^{-/-}$ DCs were higher. $Casp8^{-/-}$ BMDCs transfected with poly(I:C) showed enhanced p-IRF3 expression at 4 h compared with control BMDCs, whereas levels of total IRF3 and LaminB were similar between $Casp8^{-/-}$ and control BMDCs at 4 h (Fig. 7A).

To test whether splenic $Casp8^{-/-}$ cDCs also had enhanced p-IRF3 expression upon RIG-I stimulation, we analyzed levels of p-IRF3 in poly(I:C)-transfected CD11c$^+$ cells by flow cytometry. We found that whereas levels of p-IRF3 were not notably higher in either unstimulated (0 h) or RIG-I stimulated (4 h) CD11b$^+$ $Casp8^{-/-}$ cDCs, p-IRF3 levels were higher in a subset of CD11b$^+$ cDCs, which were also CD86$^+$, under both conditions (Fig. 7B). We infer that the CD11b$^+$ CD86$^+$ cDCs are the DCs that are either endogenously activated (0 h) or become activated after RIG-I stimulation (4 h). Thus, it appears that both $Casp8^{-/-}$ BMDCs and the activated subset of $Casp8^{-/-}$ splenic cDCs upregulate P-IRF3 to a greater degree compared with controls.

Of note, control and $Casp8^{-/-}$ CD8$^+$ splenic cDCs expressed similar levels of p-IRF3, regardless of whether they were transfected with poly(I:C) (data not shown). One explanation is the very low expression of RIG-I in CD8$^+$ DCs and the lack of IFN-α production by this DC subset in response to infection with two RNA viruses, Sendai virus, or influenza A virus (59), indicating that CD8$^+$ DCs do not use RIG-I to detect viral RNA.

Discussion

Although DCs represent a small proportion of total immune cells, they are essential for both initiating and preventing adaptive immune responses. These seemingly paradoxical outcomes depend in large part on whether the DCs are activated. Immature, unactivated DCs help prevent autoimmunity by presenting self-antigens to self-reactive T cells that have escaped thymic deletion, and such T cells are either deleted or become anergic (60). If mature DCs present oligopeptides to T cells, the result is T cell activation and proliferation such that in principle, presentation of a self-peptide by a mature DC could result in an autoimmune response (6). The fact that T cells require activated, mature DCs (induced through exposure to adjuvant or by pathogen-recognition receptor signaling) constitutes the basis for "the immunologist's dirty little secret" as presciently described by Janeway (61). A surprising aspect of the present work is that CASP8 exerts a quantitatively modest effect on the activation status and cytokine production of DCs, and yet, $Casp8$ deletion in DCs is sufficient to push the immune system into a state of self-reactivity as well as affect the progression of a persistent viral infection. This highlights the notion that immune regulation balances on a knife-edge between self-reactivity and effective immunity. As it is presently evolved, there appears to be little margin for the further enhanced effectiveness of adaptive immunity.

The importance of DCs in mediating self-tolerance is illustrated in mouse models of constitutive DC ablation. CD11c-DTA mice, which primarily lack DCs (but also certain macrophages, NK cells, and activated T cells), display impaired CD4$^+$ and CD8$^+$ T cell responses, and in one study they developed steady-state autoimmunity characterized by CD4$^+$ T cell activation (62). When DCs

(**E**) The expression of CD95 and GL-7 in B cells was assessed, and the percentage of CD95$^+$GL-7$^+$ cells is depicted (right). The percentage of MHCII$^+$ CD138$^+$ and CXCR4$^+$CD138$^+$ cells in the spleen is also depicted (bottom). (**F**) ELISAs were performed to determine the amount of LCMV-specific IgG, IgG1, and IgG2a Abs in serum. Data for (A), (D), and (E) show the average of at least 12 individual mice per group taken from two independent experiments. Data for (B) depict 8 pooled mice per group (days 8 and 15 p.i.) and 20 pooled mice per group (day 30 p.i.) from two to three independent experiments. Data for (C) depict eight pooled mice per group from two independent experiments. Data for (F) are representative of two independent experiments, with $n = 4$. Error bars represent SEM (A–E) and SD (F). *$p \leq 0.05$, **$p \leq 0.01$, ***$p \leq 0.001$, ****$p \leq 0.0001$.
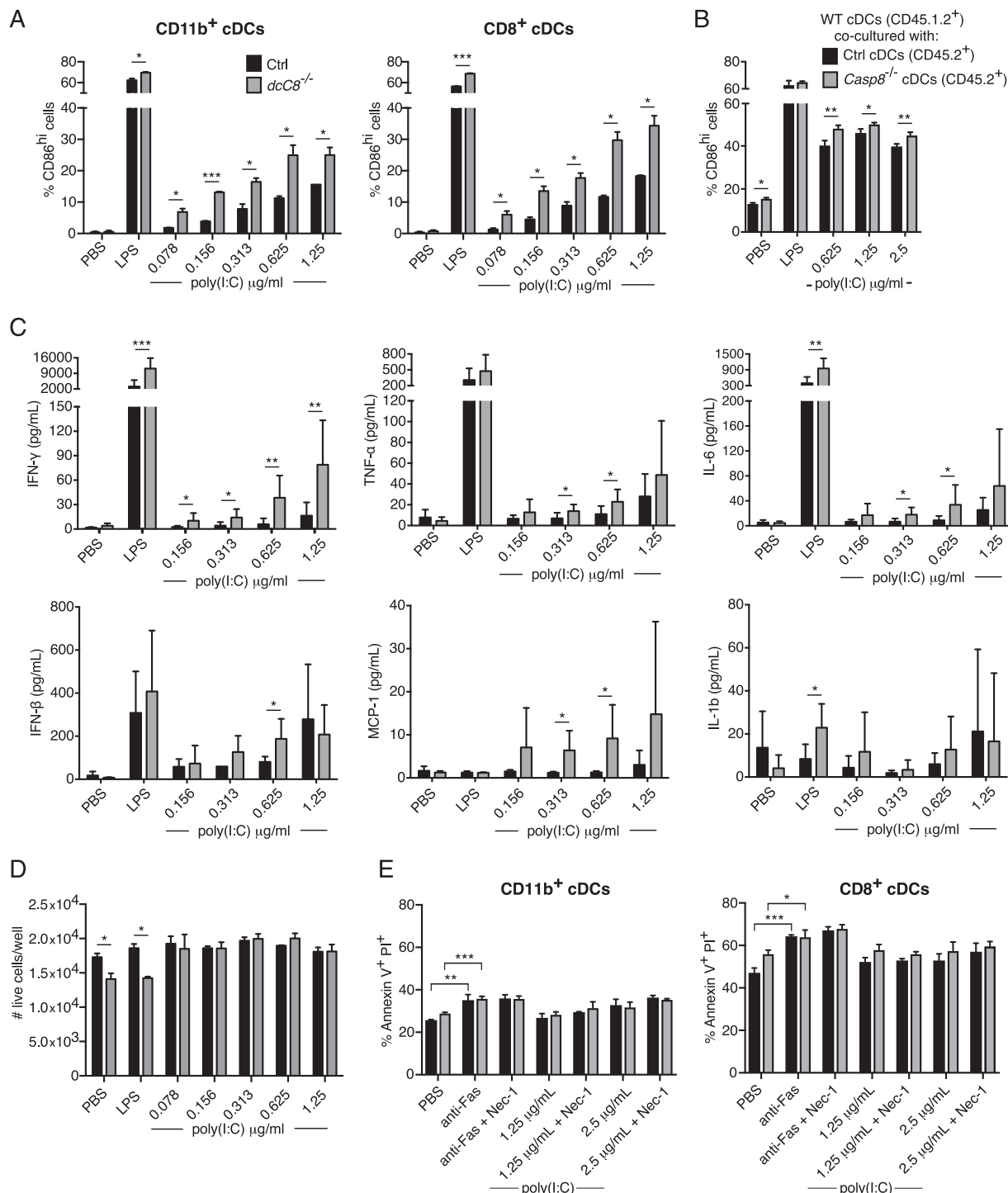
FIGURE 6. CASP8-deficient cDCs hyperactivate in response to RIG-I stimulation. (**A**) CD11c+ spleen cells were transfected with short-length poly(I:C) for 20 h, and the expression of CD86 was assessed in CD11b+ and CD8+ cDCs. (**B**) CD45.1.2+ WT CD11c+ cells were cocultured with CD45.2+ control or *Casp8*−/− CD11c+ cells in the presence of transfected short-length poly(I:C), and after 16 h assessed for the expression of CD86. (**C**) CD11c+ cells were isolated from the spleen and transfected with short-length poly(I:C) for 20 h, and levels of proinflammatory cytokines were measured in the cell supernatant by cytometric bead assay. (**D**) The number of live cDCs from (A) was assessed by labeling with an amine-reactive dye. (**E**) CD11c+ cells were isolated from the spleen and either stimulated with anti-Fas or transfected with short-length poly(I:C) for 16 h, with or without Nec-1 pretreatment. CD11b+ and CD8+ cDCs were then labeled with annexin V and PI to measure cell death. Data for (A), (B), and (D) are representative of three independent experiments, with three replicates per genotype. Data for (C) are representative of two independent experiments, with two replicates per genotype. Data for (E) are representative of two independent experiments, with three replicates per genotype. Error bars represent SD. *$p \leq 0.05$, **$p \leq 0.01$, ***$p \leq 0.001$.
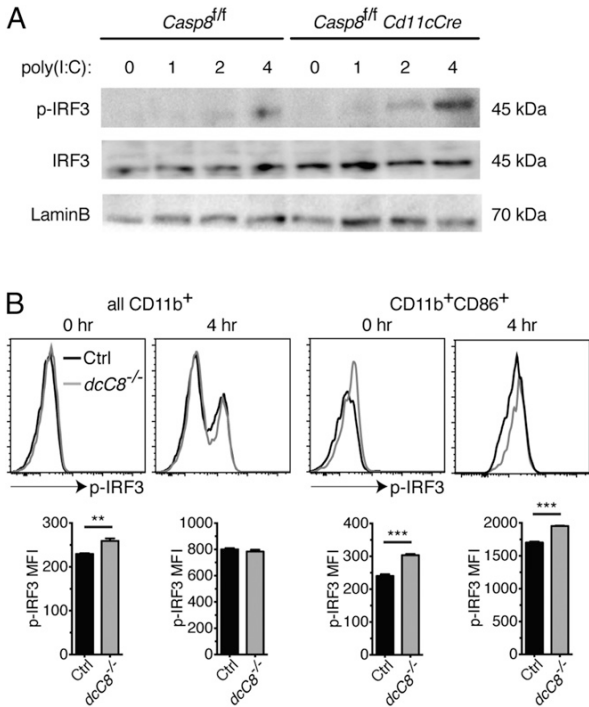
FIGURE 7. Enhanced IRF3 activation in RIG-I stimulated CASP8-deficient BMDCs and splenic cDCs. (**A**) Control and *Casp8*fl/fl *Cd11cCre* BMDCs were transfected with short-length poly(I:C) for the indicated lengths of time, then total cellular lysates were immunoblotted for p-IRF3. The membrane was then stripped and reblotted for total IRF3 and LaminB as a loading control. (**B**) CD11c⁺ cells were isolated from the spleen and transfected with short-length poly(I:C). After 4 h, the expression of p-IRF3 was assessed in CD11b⁺ and CD11b⁺CD86⁺ cDCs. Data for (A) are representative of two independent experiments. Data for (B) are representative of two independent experiments, with three replicates per genotype per experiment. Error bars represent SD. $*p \leq 0.05$, $**p \leq 0.01$, $***p \leq 0.001$.

are constitutively deleted from lupus-prone *MRL.Fas*lpr mice, age-dependent T cell expansion and differentiation into IFN-γ–producing effector cells was diminished, leading to disease reduction (63). However, when activated DCs are unable to be eliminated via Fas-mediated killing, systemic autoimmunity developed (41).

Several genes have been identified as negative regulators of DC activation; for example, mice with DC-specific ablations of A20 or SHP1 spontaneously developed mature DCs that produced more inflammatory cytokines and drove the increased activation and differentiation of T cells (6). The effect of deleting a DC-negative regulator on the viral immune response in vivo is less clear. CASP8 is a negative regulator of RIG-I signaling, a key pathway for detection of RNA viruses in DCs (10, 33). Mice with a DC-specific ablation of *Casp8* have previously been shown to develop an age-dependent autoimmunity that depends on TLR signaling (32). We show in this study that stimulated CD4⁺ T cells from aged *dcCasp8*⁻/⁻ mice skew toward a Th1 phenotype, indicating a possible role for IFN-γ in disease pathogenesis. We further explored the consequences of hyperactive DCs in the context of a chronic viral infection. These experiments revealed an adjuvant-like effect with the loss of *Casp8* in DCs, as *dcCasp8*⁻/⁻ mice have an enhanced immune response to LCMV Cl13, an RNA virus detected by RIG-I. The observation that hyperactive DCs can aid in the resolution of chronic viral infection, despite their damaging role in driving steady-state autoimmunity, is consistent with the finding that although mice with Fas-deficient DCs

develop systemic autoimmunity, they also clear a chronic LCMV infection more rapidly (41, 64).

Over time, *dcCasp8*⁻/⁻ mice develop systemic autoimmunity in the absence of external pathogen challenge. This suggests that peripheral tolerance depends upon the precise regulation of DC activation, and self-tolerance is lost with even a modest imbalance in innate signaling. *dcCasp8*⁻/⁻ mice would be expected to display enhanced Ag presentation to naive T cells, and this was borne out in experiments in which LCMV-specific CD4 T cells (SMARTA) were transferred into either control or *dcCasp8*⁻/⁻ mice. This finding supports the idea that the enhanced early CD4⁺ T cell response in LCMV Cl13 infected *dcCasp8*⁻/⁻ mice is likely due to the superefficient cDCs and not pre-existing hyperactivated T cells. In contrast, the enhanced CD8⁺ T cell response found later (days 15 and 30 p.i.) may or may not result from *Casp8*-deficient DCs. Given that a greater proportion of Ag-specific CD4⁺ T cells in *dcCasp8*⁻/⁻ mice are polyfunctional, one possibility is that the CD8⁺ T cells in infected *dcCasp8*⁻/⁻ mice receive more help from CD4⁺ T cells (50, 52).

We predicted that *Casp8*-deficient cDCs are hypersensitive to RIG-I stimulation, and we found that *Casp8*⁻/⁻ cDCs upregulated CD86 to a greater degree than control cDCs upon transfection with poly(I:C). We also predicted that a loss of *Casp8* in cDCs would lead to hyperactive IRF3 and increased IFN-I production, and although the increase in IFN-β secretion by RIG-I stimulated *Casp8*⁻/⁻ cDCs was only significant at a single concentration of transfected poly(I:C) (Fig. 6C), we found that *Casp8*⁻/⁻ BMDCs had enhanced IRF3 activation as measured by p-IRF3 (Fig. 7A). Exposure to IFN-I not only leads to DC activation, including upregulation of costimulatory molecules such as CD86 and CD80, but has also been shown to increase IFN-γ and TNF-α production by DCs (65–68). Thus, the enhanced activation of IRF3 in poly(I:C)-transfected *Casp8*⁻/⁻ DCs appears to lead to slightly higher levels of IFN-β production, which could act in an autocrine fashion on DCs to promote proinflammatory cytokine production and T cell stimulation.

If enhanced IRF3 activation in *Casp8*⁻/⁻ cDCs was responsible for the observed DC hyperactivation, we might expect that deleting IRF3 in *dcCasp8*⁻/⁻ mice would ameliorate this phenotype. Perhaps surprisingly, one group found that *IRF3*⁻/⁻ *dcCasp8*⁻/⁻ mice instead had exacerbated lymphoproliferation compared with *dcCasp8*⁻/⁻ mice (32). However, the *IRF3*⁻/⁻ *dcCasp8*⁻/⁻ mice analyzed in this study had a germline deletion of IRF3, indicating that the contributions of IRF3-deficient non-DCs to accelerating lymphoproliferation cannot be ruled out.

Unlike in many other cell types, *Casp8* deficiency in DCs does not appear to potentiate necroptosis. CASP8 is needed to both prevent necroptosis of proliferating T cells during the initiation of an adaptive immune response, as well as trigger apoptosis of T cells during the contraction of the response (27, 28, 69). However, RIG-I–stimulated control and *Casp8*⁻/⁻ cDCs underwent comparable levels of annexin V⁺PI⁺ cell death regardless of whether Nec-1 was added, indicating a RIPK1-independent root cause of the phenotypes observed in *dcCasp8*⁻/⁻ mice. Additionally, although we found that *Casp8*⁻/⁻ cDCs secreted increased amounts of IL-1β upon LPS treatment, consistent with two previous studies (31, 32), there was no difference in IL-1β production from poly(I:C)-transfected cDCs. We conclude that our findings are consistent with studies showing that deletion of *Casp8* in DCs leads to hyperactivation of downstream elements (31–34). In addition, this hyperactivation would appear to be RIPK1 and IL-1β independent.

Finally, we found that mice with hyperactive DCs lacking *Casp8* have delayed T cell exhaustion during chronic LCMV infection, indicating a possible therapeutic application for these DCs. T cell

exhaustion is characterized by a loss of effector cytokine production and upregulation of inhibitory receptors such as PD-1 and CTLA-4, and it plays a major role in disease progression of many chronic infections and cancer (45, 46). Given the role of therapeutic checkpoint inhibitors that block these T cell inhibitory pathways to enhance antitumor immunity, we speculate that enhancing DC function, even modestly, could have a major impact on the course of an immune response.

Acknowledgments

Disclosures

The authors have no financial conflicts of interest.

References

1. Steinman, R. M. 2012. Decisions about dendritic cells: past, present, and future. *Annu. Rev. Immunol.* 30: 1–22.
2. Merad, M., P. Sathe, J. Helft, J. Miller, and A. Mortha. 2013. The dendritic cell lineage: ontogeny and function of dendritic cells and their subsets in the steady state and the inflamed setting. *Annu. Rev. Immunol.* 31: 563–604.
3. Wilson, N. S., D. El-Sukkari, G. T. Belz, C. M. Smith, W. R. Heath, K. Shortman, and J. A. Villadangos. 2003. Most lymphoid organ dendritic cell types are phenotypically and functionally immature. *Blood* 102: 2187–2194.
4. Hawiger, D., K. Inaba, Y. Dorsett, M. Guo, K. Mahnke, M. Rivera, J. V. Ravetch, R. M. Steinman, and M. C. Nussenzweig. 2001. Dendritic cells induce peripheral T cell unresponsiveness under steady state conditions in vivo. *J. Exp. Med.* 194: 769–779.
5. Yamazaki, S., T. Iyoda, K. Tarbell, K. Olson, K. Velinzon, K. Inaba, and R. M. Steinman. 2003. Direct expansion of functional CD25+ CD4+ regulatory T cells by antigen-processing dendritic cells. *J. Exp. Med.* 198: 235–247.
6. Ganguly, D., S. Haak, V. Sisirak, and B. Reizis. 2013. The role of dendritic cells in autoimmunity. *Nat. Rev. Immunol.* 13: 566–577.
7. Crispín, J. C., M. I. Vargas-Rojas, A. Monsiváis-Urenda, and J. Alcocer-Varela. 2012. Phenotype and function of dendritic cells of patients with systemic lupus erythematosus. *Clin. Immunol.* 143: 45–50.
8. Iwasaki, A., and R. Medzhitov. 2015. Control of adaptive immunity by the innate immune system. *Nat. Immunol.* 16: 343–353.
9. Yoneyama, M., M. Kikuchi, T. Natsukawa, N. Shinobu, T. Imaizumi, M. Miyagishi, K. Taira, S. Akira, and T. Fujita. 2004. The RNA helicase RIG-I has an essential function in double-stranded RNA-induced innate antiviral responses. *Nat. Immunol.* 5: 730–737.
10. Kato, H., S. Sato, M. Yoneyama, M. Yamamoto, S. Uematsu, K. Matsui, T. Tsujimura, K. Takeda, T. Fujita, O. Takeuchi, and S. Akira. 2005. Cell type-specific involvement of RIG-I in antiviral response. *Immunity* 23: 19–28.
11. Fitzgerald, K. A., S. M. McWhirter, K. L. Faia, D. C. Rowe, E. Latz, D. T. Golenbock, A. J. Coyle, S. M. Liao, and T. Maniatis. 2003. IKKepsilon and TBK1 are essential components of the IRF3 signaling pathway. *Nat. Immunol.* 4: 491–496.
12. Sharma, S., B. R. tenOever, N. Grandvaux, G. P. Zhou, R. Lin, and J. Hiscott. 2003. Triggering the interferon antiviral response through an IKK-related pathway. *Science* 300: 1148–1151.
13. Kawai, T., K. Takahashi, S. Sato, C. Coban, H. Kumar, H. Kato, K. J. Ishii, O. Takeuchi, and S. Akira. 2005. IPS-1, an adaptor triggering RIG-I- and Mda5-mediated type I interferon induction. *Nat. Immunol.* 6: 981–988.
14. Meylan, E., J. Curran, K. Hofmann, D. Moradpour, M. Binder, R. Bartenschlager, and J. Tschopp. 2005. Cardif is an adaptor protein in the RIG-I antiviral pathway and is targeted by hepatitis C virus. *Nature* 437: 1167–1172.
15. Seth, R. B., L. Sun, C. K. Ea, and Z. J. Chen. 2005. Identification and characterization of MAVS, a mitochondrial antiviral signaling protein that activates NF-kappaB and IRF 3. *Cell* 122: 669–682.
16. Blanco, P., A. K. Palucka, M. Gill, V. Pascual, and J. Banchereau. 2001. Induction of dendritic cell differentiation by IFN-α in systemic lupus erythematosus. *Science* 294: 1540–1543.
17. González-Navajas, J. M., J. Lee, M. David, and E. Raz. 2012. Immunomodulatory functions of type I interferons. *Nat. Rev. Immunol.* 12: 125–135.
18. Vercammen, D., R. Beyaert, G. Denecker, V. Goossens, G. Van Loo, W. Declercq, J. Grooten, W. Fiers, and P. Vandenabeele. 1998. Inhibition of caspases increases the sensitivity of L929 cells to necrosis mediated by tumor necrosis factor. *J. Exp. Med.* 187: 1477–1485.
19. Holler, N., R. Zaru, O. Micheau, M. Thome, A. Attinger, S. Valitutti, J. L. Bodmer, P. Schneider, B. Seed, and J. Tschopp. 2000. Fas triggers an alternative, caspase-8-independent cell death pathway using the kinase RIP as effector molecule. *Nat. Immunol.* 1: 489–495.
20. Degterev, A., J. Hitomi, M. Germscheid, I. L. Ch'en, O. Korkina, X. Teng, D. Abbott, G. D. Cuny, C. Yuan, G. Wagner, et al. 2008. Identification of RIP1 kinase as a specific cellular target of necrostatins. *Nat. Chem. Biol.* 4: 313–321.
21. Cho, Y. S., S. Challa, D. Moquin, R. Genga, T. D. Ray, M. Guildford, and F. K. Chan. 2009. Phosphorylation-driven assembly of the RIP1-RIP3 complex regulates programmed necrosis and virus-induced inflammation. *Cell* 137: 1112–1123.
22. He, S., L. Wang, L. Miao, T. Wang, F. Du, L. Zhao, and X. Wang. 2009. Receptor interacting protein kinase-3 determines cellular necrotic response to TNF-alpha. *Cell* 137: 1100–1111.
23. Zhang, D. W., J. Shao, J. Lin, N. Zhang, B. J. Lu, S. C. Lin, M. Q. Dong, and J. Han. 2009. RIP3, an energy metabolism regulator that switches TNF-induced cell death from apoptosis to necrosis. *Science* 325: 332–336.
24. Kaiser, W. J., J. W. Upton, A. B. Long, D. Livingston-Rosanoff, L. P. Daley-Bauer, R. Hakem, T. Caspary, and E. S. Mocarski. 2011. RIP3 mediates the embryonic lethality of caspase-8-deficient mice. *Nature* 471: 368–372.
25. Oberst, A., C. P. Dillon, R. Weinlich, L. L. McCormick, P. Fitzgerald, C. Pop, R. Hakem, G. S. Salvesen, and D. R. Green. 2011. Catalytic activity of the caspase-8-FLIP(L) complex inhibits RIPK3-dependent necrosis. *Nature* 471: 363–367.
26. Varfolomeev, E. E., M. Schuchmann, V. Luria, N. Chiannilkulchai, J. S. Beckmann, I. L. Mett, D. Rebrikov, V. M. Brodianski, O. C. Kemper, O. Kollet, et al. 1998. Targeted disruption of the mouse Caspase 8 gene ablates cell death induction by the TNF receptors, Fas/Apo1, and DR3 and is lethal prenatally. *Immunity* 9: 267–276.
27. Ch'en, I. L., D. R. Beisner, A. Degterev, C. Lynch, J. Yuan, A. Hoffmann, and S. M. Hedrick. 2008. Antigen-mediated T cell expansion regulated by parallel pathways of death. *Proc. Natl. Acad. Sci. USA* 105: 17463–17468.
28. Ch'en, I. L., J. S. Tsau, J. D. Molkentin, M. Komatsu, and S. M. Hedrick. 2011. Mechanisms of necroptosis in T cells. *J. Exp. Med.* 208: 633–641.
29. Günther, C., E. Martini, N. Wittkopf, K. Amann, B. Weigmann, H. Neumann, M. J. Waldner, S. M. Hedrick, S. Tenzer, M. F. Neurath, and C. Becker. 2011. Caspase-8 regulates TNF-α-induced epithelial necroptosis and terminal ileitis. *Nature* 477: 335–339.
30. Ofengeim, D., Y. Ito, A. Najafov, Y. Zhang, B. Shan, J. P. DeWitt, J. Ye, X. Zhang, A. Chang, H. Vakifahmetoglu-Norberg, et al. 2015. Activation of necroptosis in multiple sclerosis. *Cell Reports* 10: 1836–1849.
31. Kang, T. B., S. H. Yang, B. Toth, A. Kovalenko, and D. Wallach. 2013. Caspase-8 blocks kinase RIPK3-mediated activation of the NLRP3 inflammasome. *Immunity* 38: 27–40.
32. Cuda, C. M., A. V. Misharin, A. K. Gierut, R. Saber, G. K. Haines, III, J. Hutcheson, S. M. Hedrick, C. Mohan, G. S. Budinger, C. Stehlik, and H. Perlman. 2014. Caspase-8 acts as a molecular rheostat to limit RIPK1- and MyD88-mediated dendritic cell activation. *J. Immunol.* 192: 5548–5560.
33. Rajput, A., A. Kovalenko, K. Bogdanov, S. H. Yang, T. B. Kang, J. C. Kim, J. Du, and D. Wallach. 2011. RIG-I RNA helicase activation of IRF3 transcription factor is negatively regulated by caspase-8-mediated cleavage of the RIP1 protein. *Immunity* 34: 340–351.
34. Sears, N., G. C. Sen, G. R. Stark, and S. Chattopadhyay. 2011. Caspase-8-mediated cleavage inhibits IRF-3 protein by facilitating its proteasome-mediated degradation. *J. Biol. Chem.* 286: 33037–33044.
35. Cuda, C. M., A. V. Misharin, S. Khare, R. Saber, F. Tsai, A. M. Archer, P. J. Homan, G. K. Haines, III, J. Hutcheson, A. Dorfleutner, et al. 2015. Conditional deletion of caspase-8 in macrophages alters macrophage activation in a RIPK-dependent manner. *Arthritis Res. Ther.* 17: 291–307.
36. Beisner, D. R., I. L. Ch'en, R. V. Kolla, A. Hoffmann, and S. M. Hedrick. 2005. Cutting edge: innate immunity conferred by B cells is regulated by caspase-8. *J. Immunol.* 175: 3469–3473.
37. Caton, M. L., M. R. Smith-Raska, and B. Reizis. 2007. Notch-RBP-J signaling controls the homeostasis of CD8- dendritic cells in the spleen. *J. Exp. Med.* 204: 1653–1664.
38. Oxenius, A., M. F. Bachmann, R. M. Zinkernagel, and H. Hengartner. 1998. Virus-specific MHC-class II-restricted TCR-transgenic mice: effects on humoral and cellular immune responses after viral infection. *Eur. J. Immunol.* 28: 390–400.
39. Ahmed, R., A. Salmi, L. D. Butler, J. M. Chiller, and M. B. Oldstone. 1984. Selection of genetic variants of lymphocytic choriomeningitis virus in spleens of persistently infected mice. Role in suppression of cytotoxic T lymphocyte response and viral persistence. *J. Exp. Med.* 160: 521–540.
40. Harker, J. A., G. M. Lewis, L. Mack, and E. I. Zuniga. 2011. Late interleukin-6 escalates T follicular helper cell responses and controls a chronic viral infection. *Science* 334: 825–829.
41. Stranges, P. B., J. Watson, C. J. Cooper, C. M. Choisy-Rossi, A. C. Stonebraker, R. A. Beighton, H. Hartig, J. P. Sundberg, S. Servick, G. Kaufmann, et al. 2007. Elimination of antigen-presenting cells and autoreactive T cells by Fas contributes to prevention of autoimmunity. *Immunity* 26: 629–641.
42. Harigai, M., M. Kawamoto, M. Hara, T. Kubota, N. Kamatani, and N. Miyasaka. 2008. Excessive production of IFN-gamma in patients with systemic lupus erythematosus and its contribution to induction of B lymphocyte stimulator/B cell-activating factor/TNF ligand superfamily-13B. *J. Immunol.* 181: 2211–2219.
43. Clingan, J. M., K. Ostrow, K. A. Hosiawa, Z. J. Chen, and M. Matloubian. 2012. Differential roles for RIG-I-like receptors and nucleic acid-sensing TLR pathways in controlling a chronic viral infection. *J. Immunol.* 188: 4432–4440.
44. Wherry, E. J., J. N. Blattman, K. Murali-Krishna, R. van der Most, and R. Ahmed. 2003. Viral persistence alters CD8 T-cell immunodominance and tissue distribution and results in distinct stages of functional impairment. *J. Virol.* 77: 4911–4927.
45. Wherry, E. J., S. J. Ha, S. M. Kaech, W. N. Haining, S. Sarkar, V. Kalia, S. Subramaniam, J. N. Blattman, D. L. Barber, and R. Ahmed. 2007. Molecular signature of CD8+ T cell exhaustion during chronic viral infection. *Immunity* 27: 670–684.
46. Crawford, A., J. M. Angelosanto, C. Kao, T. A. Doering, P. M. Odorizzi, B. E. Barnett, and E. J. Wherry. 2014. Molecular and transcriptional basis of CD4+ T cell dysfunction during chronic infection. *Immunity* 40: 289–302.
47. Barber, D. L., E. J. Wherry, D. Masopust, B. Zhu, J. P. Allison, A. H. Sharpe, G. J. Freeman, and R. Ahmed. 2006. Restoring function in exhausted CD8 T cells during chronic viral infection. *Nature* 439: 682–687.

48. Doedens, A. L., A. T. Phan, M. H. Stradner, J. K. Fujimoto, J. V. Nguyen, E. Yang, R. S. Johnson, and A. W. Goldrath. 2013. Hypoxia-inducible factors enhance the effector responses of CD8(+) T cells to persistent antigen. *Nat. Immunol.* 14: 1173–1182.

49. Sevilla, N., D. B. McGavern, C. Teng, S. Kunz, and M. B. Oldstone. 2004. Viral targeting of hematopoietic progenitors and inhibition of DC maturation as a dual strategy for immune subversion. *J. Clin. Invest.* 113: 737–745.

50. Elsaesser, H., K. Sauer, and D. G. Brooks. 2009. IL-21 is required to control chronic viral infection. *Science* 324: 1569–1572.

51. Fröhlich, A., J. Kisielow, I. Schmitz, S. Freigang, A. T. Shamshiev, J. Weber, B. J. Marsland, A. Oxenius, and M. Kopf. 2009. IL-21R on T cells is critical for sustained functionality and control of chronic viral infection. *Science* 324: 1576–1580.

52. Yi, J. S., M. Du, and A. J. Zajac. 2009. A vital role for interleukin-21 in the control of a chronic viral infection. *Science* 324: 1572–1576.

53. Baumjohann, D., S. Preite, A. Reboldi, F. Ronchi, K. M. Ansel, A. Lanzavecchia, and F. Sallusto. 2013. Persistent antigen and germinal center B cells sustain T follicular helper cell responses and phenotype. *Immunity* 38: 596–605.

54. Nutt, S. L., P. D. Hodgkin, D. M. Tarlinton, and L. M. Corcoran. 2015. The generation of antibody-secreting plasma cells. *Nat. Rev. Immunol.* 15: 160–171.

55. Tishon, A., H. Lewicki, G. Rall, M. Von Herrath, and M. B. Oldstone. 1995. An essential role for type 1 interferon-gamma in terminating persistent viral infection. *Virology* 212: 244–250.

56. Luzina, I. G., S. P. Atamas, C. E. Storrer, L. C. daSilva, G. Kelsoe, J. C. Papadimitriou, and B. S. Handwerger. 2001. Spontaneous formation of germinal centers in autoimmune mice. *J. Leukoc. Biol.* 70: 578–584.

57. Kato, H., O. Takeuchi, E. Mikamo-Satoh, R. Hirai, T. Kawai, K. Matsushita, A. Hiiragi, T. S. Dermody, T. Fujita, and S. Akira. 2008. Length-dependent recognition of double-stranded ribonucleic acids by retinoic acid-inducible gene-I and melanoma differentiation-associated gene 5. *J. Exp. Med.* 205: 1601–1610.

58. Sauter, B., M. L. Albert, L. Francisco, M. Larsson, S. Somersan, and N. Bhardwaj. 2000. Consequences of cell death: exposure to necrotic tumor cells, but not primary tissue cells or apoptotic cells, induces the maturation of immunostimulatory dendritic cells. *J. Exp. Med.* 191: 423–434.

59. Luber, C. A., J. Cox, H. Lauterbach, B. Fancke, M. Selbach, J. Tschopp, S. Akira, M. Wiegand, H. Hochrein, M. O'Keeffe, and M. Mann. 2010. Quantitative proteomics reveals subset-specific viral recognition in dendritic cells. *Immunity* 32: 279–289.

60. Steinman, R. M., D. Hawiger, and M. C. Nussenzweig. 2003. Tolerogenic dendritic cells. *Annu. Rev. Immunol.* 21: 685–711.

61. Janeway, C. A., Jr. 1989. Approaching the asymptote? Evolution and revolution in immunology. *Cold Spring Harb. Symp. Quant. Biol.* 54: 1–13.

62. Ohnmacht, C., A. Pullner, S. B. King, I. Drexler, S. Meier, T. Brocker, and D. Voehringer. 2009. Constitutive ablation of dendritic cells breaks self-tolerance of CD4 T cells and results in spontaneous fatal autoimmunity. *J. Exp. Med.* 206: 549–559.

63. Teichmann, L. L., M. L. Ols, M. Kashgarian, B. Reizis, D. H. Kaplan, and M. J. Shlomchik. 2010. Dendritic cells in lupus are not required for activation of T and B cells but promote their expansion, resulting in tissue damage. *Immunity* 33: 967–978.

64. Varanasi, V., A. A. Khan, and A. V. Chervonsky. 2014. Loss of the death receptor CD95 (Fas) expression by dendritic cells protects from a chronic viral infection. *Proc. Natl. Acad. Sci. USA* 111: 8559–8564.

65. Ito, T., R. Amakawa, M. Inaba, S. Ikehara, K. Inaba, and S. Fukuhara. 2001. Differential regulation of human blood dendritic cell subsets by IFNs. *J. Immunol.* 166: 2961–2969.

66. Parlato, S., S. M. Santini, C. Lapenta, T. Di Pucchio, M. Logozzi, M. Spada, A. M. Giammarioli, W. Malorni, S. Fais, and F. Belardelli. 2001. Expression of CCR-7, MIP-3beta, and Th-1 chemokines in type I IFN-induced monocyte-derived dendritic cells: importance for the rapid acquisition of potent migratory and functional activities. *Blood* 98: 3022–3029.

67. Montoya, M., G. Schiavoni, F. Mattei, I. Gresser, F. Belardelli, P. Borrow, and D. F. Tough. 2002. Type I interferons produced by dendritic cells promote their phenotypic and functional activation. *Blood* 99: 3263–3271.

68. Montoya, M., M. J. Edwards, D. M. Reid, and P. Borrow. 2005. Rapid activation of spleen dendritic cell subsets following lymphocytic choriomeningitis virus infection of mice: analysis of the involvement of type 1 IFN. *J. Immunol.* 174: 1851–1861.

69. Hedrick, S. M., I. L. Ch'en, and B. N. Alves. 2010. Intertwined pathways of programmed cell death in immunity. *Immunol. Rev.* 236: 41–53.